Catal Lett (2009) 128:268–280
DOI 10.1007/s10562-008-9695-y

Influence of the Support Treatment on the Behavior of $MnOx/Al_2O_3$ Catalysts used in VOC Combustion

Fabiola N. Aguero · Alberto Scian · Bibiana P. Barbero · Luis E. Cadús

Received: 28 July 2008 / Accepted: 22 September 2008 / Published online: 15 October 2008

Abstract Alumina was treated with water and diluted nitric acid and then was used to prepare supported MnO_x/Al_2O_3 catalysts with two different loadings. The influence of the support treatment on the catalytic behavior in ethanol and toluene combustion was studied. The treatments modified the alumina physicochemical properties (porosity, surface area, isoelectric point, and surface acidity). The modification of these properties affected the interaction of the manganese oxide species with the support and increased the dispersion of the active phase. Catalysts prepared from treated supports showed the best catalytic performance in ethanol combustion. At high manganese loading, this better catalytic performance was related to the high capacity for adsorbing oxygen. While at low manganese loading, the great amount of dispersed surface manganese oxide species and/or the existence of surface defects were relevant in the catalytic activity. On the other hand, the reactivity of the catalysts in toluene combustion was roughly correlated with the reducibility of the surface manganese oxide species. On the basis of these observations, we conclude that the ethanol combustion occurs by a suprafacial mechanism whereas the toluene combustion proceeds through an intrafacial mechanism.

F. N. Aguero (✉) · B. P. Barbero · L. E. Cadús
Instituto de Investigaciones en Tecnología Química (INTEQUI), UNSL - CONICET, Casilla de Correo 290, 5700 San Luis, Argentina
e-mail: naguero@fices.unsl.edu.ar

A. Scian
Centro de Tecnología de Recursos Minerales y Cerámica (CETMIC), Camino Parque Centenario y 506, 1897 Manuel B. Gonnet, (Buenos Aires), Argentina

Keywords Alumina · Manganese oxide · Support treatment · Total oxidation · VOC

1 Introduction

Total catalytic oxidation technology is widely used in several industrial processes for air pollution abatement, especially for control of volatile organic compound emissions [1]. Compared with thermal combustion techniques higher efficiencies at lower operating temperatures are reached, obtaining considerable environment and economic benefits [2].

Catalysts used in total oxidation reactions are supported noble metals (platinum, palladium, rhodium) and transition metal oxides or mixed metal oxides as bulk or supported catalysts [3–5]. In general the supported noble metals catalysts exhibit higher catalytic activities at lower reaction temperatures in comparison with the mixed oxide catalysts [6]. Disadvantages of these catalysts are the higher costs, the sensitivity to poisons and sintering at high temperatures [7–10]. The manganese oxides [11, 12] including bulk MnO_2, Mn_2O_3 and Mn_3O_4, as well as supported on carriers such as silica, alumina, titania, and zirconia, [13, 14] are a cheaper alternative in environmental catalysis.

Zaki et al. [15] have shown that the thermal decomposition of MnO_2 on oxidizing (O_2, air) and non oxidizing (N_2) gas atmospheres starts at 550–600 °C and results eventually in the formation of Mn_3O_4. The decomposition course of MnO_2 into Mn_3O_4 is mediated by the formation and decomposition of Mn_5O_8 and subsequently Mn_2O_3. This Mn_2O_3 is a stable phase. On an alumina support MnO_2 is formed mainly below 430 °C and Mn_2O_3 is formed at 630 °C [16, 17].

Alumina has been widely used as support of heterogeneous catalysts on several industrial applications. In last years, structured supports that treat great volumes of gases avoiding high pressure drops are being developed. These structures as monoliths usually made of ceramic or metallic materials are generally covered with an alumina layer that acts as the support of the active phase [18]. The main objective to deposit an active phase on a support oxide is to increase the exposed surface area. However, the texture and chemical properties of support have important influence on the reducibility, dispersion of the active phase and its interaction with the support and therefore on the activity and product selectivity of catalyst.

The main sources of volatile organic compounds are mobile sources from vehicles and stationary sources mainly from industries that use solvents. Among the hydrocarbons emitted in printing industries ethanol and toluene are normally present. Thus, it is interesting to evaluated the catalytic behavior in the combustion of these VOCs since they are considered to be in the extremes of reactivity [19].

In this work the effects on the catalytic activity of MnO_x/Al_2O_3 catalysts in ethanol and toluene combustion after the modification of physical and chemical properties of the support by means of treatments with water and nitric acid, were investigated.

2 Experimental

2.1 Supports Preparation

Al_2O_3: An aluminium acetate gel was prepared by a chemical reaction between pseudobohemite AlO(OH) and acetic acid in excess (11% above the stoichiometric rate) The reaction was carried out at ambient conditions in aqueous alcoholic medium. The weight ratio of the three components was: gel/H_2O/alcohol = 4/3/3. The gel was periodically shacked during 48 h, in order to favor the formation of small nucleus and to avoid its excessive growth. Two parts of alcohol for each part of the mixture were added. The system was kept in periodic agitation during 12 h and finally dried at 110 °C. The dried sample was calcined at 1000 °C for 10 min.

Al_2O_3-H_2O: a part of the original alumina was washed with distilled water until constant conductivity. The sample in pellets of 0.5–0.85 mm was placed in a U-tube and the water was recycled at 30 cc/min using a peristaltic pump. This procedure was repeated three times.

Al_2O_3-HNO_3: a portion of the original alumina was treated with a diluted nitric acid solution 10^{-2} M until constant pH value of the solution. The same mechanism employed to wash the alumina with water was used. This procedure was repeated three times.

2.2 Catalysts preparation

The catalysts were prepared by impregnation to incipient wetness of the supports (Al_2O_3, Al_2O_3-H_2O, and Al_2O_3-HNO_3), previously dried under vacuum at 137 °C for 3 h, with an aqueous solution of $Mn(CH_3COO)_2 \cdot 2H_2O$ with a concentration of 0.06 g/mL (Fluka). The impregnation was carried out in multiple stages with drying in between at 100 °C for 1 h. The amount of added solution was the necessary to obtain a manganese loading equivalent to one or three theoretical monolayers of MnO_x. Finally, the samples were dried at 70 °C overnight and calcined at 500 °C for 3 h. The obtained catalysts were called *x*Mn/Al_2O_3, *x*Mn/Al_2O_3-H_2O and *x*Mn/Al_2O_3-HNO_3 where $x = 1$ or 3 represents the manganese amount (equivalent amount to 1 or 3 theoretical monolayers of MnO_x).

2.3 Catalysts characterization

Isoelectric point (*IEP*): the IEP measurements were carried out in a Zeta Meter System 3.0 apparatus, using 30 mg of sample dispersed in a 10^{-3} M KCl solution. The pH was adjusted with either 10^{-2} M KOH or HCl solutions.

Ammonia temperature programmed desorption (*NH_3-TPD*)*:* a quartz tubular reactor and a TCD as detector were used. Samples of 300 mg were treated in a pure helium flow of 30 mL min^{-1}, from 30 to 700 °C at a heating rate of 20 °C/min. The adsorption step was carried out in a pure ammonia flow at room temperature for 1 h. Then, the sample was swept in pure helium for 30 min. The desorption was performed in a pure helium flow of 30 mL min^{-1}, from 30 to 700 °C at a heating rate of 10 °C min^{-1}. The acid strength distribution was determined using an arbitrary scale of acidity, considering weak, medium and strong acid sites to those related to the number of desorbed ammonia molecules from 25 to 200 °C, between 200 and 400 °C and above 400 °C, respectively. The area under the curve was integrated and considered as a measurement of total acidity. The weak, moderate and strong acidity was determined as the integrated area in the corresponding temperature range, divided by the total area and normalized by specific surface area (S_{BET}) unit.

Fourier-transform infrared (*FTIR*)*-pyridine adsorption*: Pyridine FTIR spectra were recorded in a Jasco FT/IR 5300 spectrometer. Samples of 15–20 mg were pressed into self-supporting discs and treated under vacuum (10^{-2} mbar) at 400 °C for 2 h. After cooling down at room temperature, the samples were exposed to pyridine vapor for 30 min. Then IR spectra were recorded after outgassing at 50 °C.

The amount of pyridine adsorbed was estimated using methods described by Emeis [20].

BET Specific Surface Area Measurements (*SSA*)*:* The specific surface area of the samples was calculated by the BET method from the nitrogen adsorption isotherms obtained at 77 K. A Micromeritics ASSAP 2000 apparatus was used.

X-ray fluorescence (XRF): a PW 1400 Philips instrument was used. The calibration was made with mixtures of oxides with known concentrations.

X-ray diffraction (XRD): XRD patterns were obtained by using a Rigaku diffractometer operated at 30 kV and 25 mA by employing Cu Kα radiation with Nickel filter ($\lambda = 0.15418$ nm).

Temperature programmed reduction (*TPR*): The TPR was performed in a quartz tubular reactor using a TCD as detector. Samples of 100 mg were used. The reducing gas was a mixture of 5 vol.% H_2/N_2, at a total flow rate of 30 mL min^{-1}. The temperature was increased at a rate of 5 °C min^{-1} from room temperature to 700 °C.

X-ray photoelectron spectroscopy (*XPS*): A ESCA VG Microtech equipment with a line of MgKα($h\upsilon = 1253.6$ eV) and an hemispheric analyzer with a pass energy of 25 eV was used. The pressure was kept under 10^{-9} Torr. The charge effect was corrected using as reference the Al2p peak (74.6 eV).

Temperature programmed desorption of oxygen (*O_2-TPD*): O_2-TPD experiments were performed in a quartz reactor using a TCD as detector. Samples of 500 mg were pre-treated with helium gas increasing the temperature from room temperature up to 500 °C at 10 °C min^{-1}. The samples were oxidized with a 20% O_2/He mixture at a total flow rate of 30 mL min^{-1} at 500 °C for 30 min. Then, they were cooled down to room temperature in the oxidising mixture and flushed by a stream of purified He for 30 min. The desorption was carried out in the same conditions as the pre-treatment, maintaining the temperature at 500 °C for 30 min.

2.4 Catalytic Evaluation

A glass reactor of fixed bed at atmospheric pressure was used. Data were obtained in steady state. A sample of 300 mg (0.5–0.8 mm particle diameter) diluted with glass particles of the same size in a ratio 1:5 was used. The feed was a mixture of molar ratio VOC:O_2:He = 1:20.8:78.2 at a total flow rate of 100 mL min^{-1}. The reagents and reaction products were analyzed on line by a Buck 910 gas chromatograph equipped with a Porapak T column for ethanol combustion and a Carbowax 20 M/Cromosorb W and a Carbosphere columns for toluene combustion and a thermal conductivity detector.

The conversion of VOC, X(%), was defined as:

$$X\% = \frac{\mathrm{VOC_{in}} - \mathrm{VOC_{out}}}{\mathrm{VOC_{in}}} * 100$$

where $[VOC]_{in}$ means VOC (ethanol or toluene) inlet molar concentration and $[VOC]_{out}$, the VOC outlet molar concentration.

3 Results

3.1 Specific Surface Area (S_{BET})

Support specific surface areas are presented in Table 1. Treatments with water or nitric acid modified the textural properties of the original support. The surface area of water treated alumina decreased to 79.5 m^2/g, but in the case of nitric acid-treated alumina it increased to 106.3 m^2/g. The pore volume and the pore mean diameter decreased after both treatments. Catalysts specific surface areas are presented in Table 2. From these results it may be appreciated that at low manganese loading catalysts prepared from the untreated and acid-treated supports practically conserve the support specific area, while catalysts prepared from water treated support present an increase of the specific area. At higher manganese loading a decrease of the specific surface area is observed for all catalysts.

3.2 X-ray fluorescence (XRF)

Manganese content was determined by X-ray fluorescence and the results are presented in Table 2. At low manganese loading, the measured and the theoretical values were quite close except for the untreated support. At higher manganese loading the measured values were lower than the theoretical ones, regardless of the support.

Table 1 Textural properties, acidity and IEP values of supports

Supports	S_{BET} (m^2/g)	Average diameter (nm)	Pore volume (ml/g)	Isoelectric point (IEP)	Acidity (μmol/m^2)
Al_2O_3	97.1	16.6	0.4	7.9	1.77
Al_2O_3-H_2O	79.5	13.4	0.33	8.3	1.81
Al_2O_3-HNO_3	106.3	12.6	0.35	9.0	0.45

Table 2 Specific surface area (S_{BET}), elemental composition from XRF, and hydrogen consumption from TPR

Catalysts	S_{BET} (m^2/g)	Mn content (%Mn)		H_2–TPR O/Mn ratio
		Theoretical	Experimental	
1Mn/Al_2O_3	92.8	12.5	10.0	1.49
3Mn/Al_2O_3	84.7	37.3	19.2	1.41
1Mn/Al_2O_3-H_2O	106.0	12.5	12.0	1.43
3Mn/Al_2O_3-H_2O	96.6	37.3	29.0	1.35
1Mn/Al_2O_3-HNO_3	104.5	12.5	12.7	1.43
3Mn/Al_2O_3-HNO_3	93.6	37.3	29.1	1.36

3.3 X-ray Diffraction (XRD)

The X-ray diffractogram of the Al_2O_3 support, see Fig. 1, shows only the transition phase θ-δ-Al_2O_3 (PDF 4-877 and 35–121). The structure of the original alumina was unchanged after the treatments. The diffractograms of the supported manganese catalysts are shown in Fig. 1. The XRD patterns of all catalysts conserved the diffraction lines of the support and exhibited additional lines corresponding to the phase Mn_2O_3 (PDF 18-803 and 24–508). The intensity of these lines increased with the manganese content. The presence of these manganese species did not modify the structure of the support.

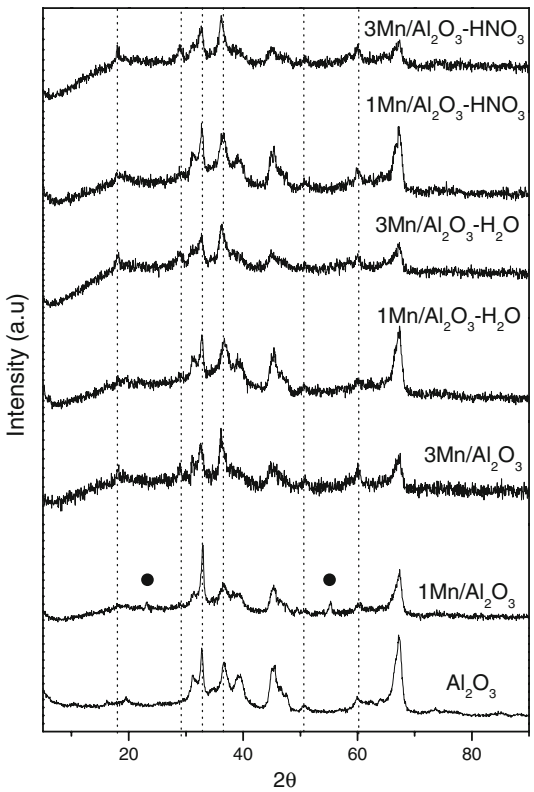

Fig. 1 X-ray diffractograms of Al_2O_3 support and manganese catalysts. (•) Mn_2O_3 JCPDS 24-508; (—) Mn_2O_3 JCPDS 18-803

3.4 Temperature Programmed Desorption of Ammonia (NH_3-TPD)

The *NH_3-TPD* results are shown in Figs. 2 and 3. The untreated Al_2O_3 TPD profile is characterized by one strong NH_3 desorption peak at about 100 °C and weaker peaks at around 250 and 425 °C. A similar curve was obtained with

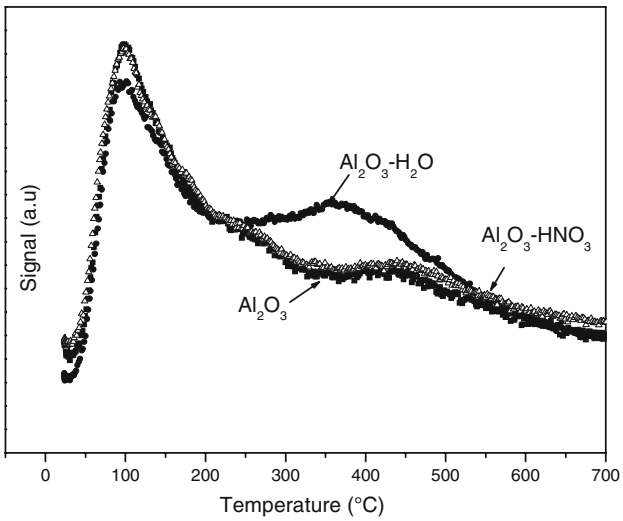

Fig. 2 Temperature programmed desorption of ammonia for the supports

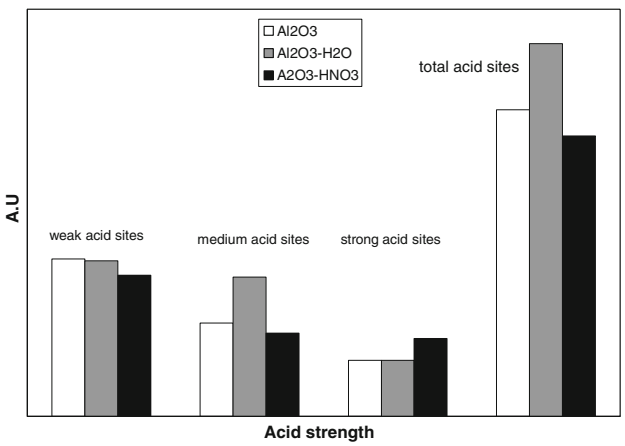

Fig. 3 Distribution of supports acid sites

nitric acid-treated alumina. However, when the support was treated with water a more intense peak at 350 °C was also observed. The acid site distribution, Fig. 3, clearly shows that total acidity of the original alumina increased with water treatment while it decreased with acid treatment. It was also observed a redistribution of acid sites with the creation of new medium acid sites when alumina was treated with water.

3.5 Fourier-Transform Infrared (FTIR)-Pyridine Adsorption

The results of FTIR-pyridine adsorption are shown in Table 1 and Fig. 4. The acid number of water treated alumina increases to 1.81 μmol/m^2. When the support is treated with nitric acid, the acid number of alumina decreases to 0.459 μmol/m^2. The supports only presented the bands at 1450, 1493, 1578, 1594, and 1614 cm^{-1} corresponding to Lewis acid sites [21]. The absence of a band around 1550 cm^{-1} indicates the lack of Bronsted acid sites.

3.6 Isoelectric Point (IEP)

The isoelectric points of Al_2O_3, Al_2O_3-H_2O and Al_2O_3-HNO_3 are shown in Table 1. Treatments with water and nitric acid increased the IEP of the original support. The IEP of catalysts shown in Table 3, decreased with the increase of manganese content, except for 3Mn/Al_2O_3-H_2O catalyst. From the IEP results, the fractional surface areas covered by Mn_2O_3, also called apparent surface coverage (ASC), were calculated using the equation presented by Gil-Llambias et al. [22]. The ASC values presented in Table 3 showed that at low manganese loading the surface coverage was similar independently on the support

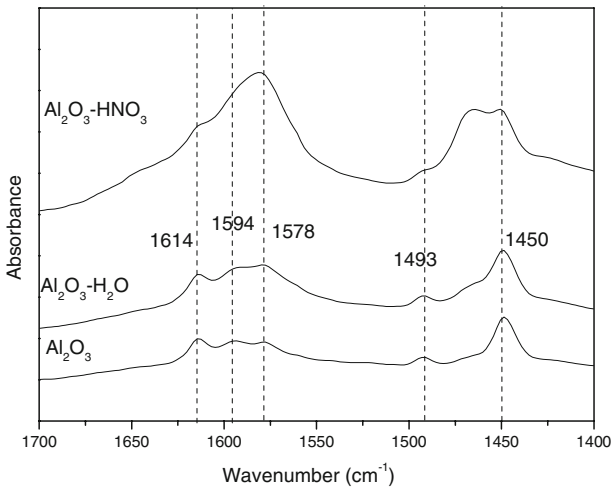

Fig. 4 FTIR spectra of adsorbed pyridine after desorption at 50 °C

treatment. However, at higher manganese loading the surface coverage increased when the support was previously treated.

3.7 X-ray Photoelectron Spectroscopy (XPS)

XPS results are presented in Table 3 and Fig. 5. For catalysts with low manganese loading, Mn2p/Al2p atomic ratios slightly decrease when catalysts are prepared from treated supports. While at higher manganese content, these atomic ratios increase when catalysts were prepared from treated supports, (0.15, 0.39 and 0.48 for 3Mn/Al_2O_3, 3Mn/Al_2O_3-H_2O, 3Mn/Al_2O_3-HNO_3 respectively). In general the Mn2p photoelectron binding energy values agreed with the literature [23]. Figure 5 shows Mn2p3/2 XPS peak of catalysts with low manganese loading instead of those with higher manganese loading because the sensitivity of the measurement of electron binding energy shift related to surface interactions is decreased with increasing loading [24]. The binding energy of the Mn2p3/2 of catalyst from the untreated support is lower than those observed for the treated supported catalysts. By deconvolution the O1 s peak, three components with binding energies at about 528.6 eV, ascribed to the lattice oxygen species (O_l), 530.6 eV, assigned to adsorbed oxygen species, (O_{ad}) [25, 26], and 532.7–533.0 eV, corresponding to water adsorbed on the surface [27, 28] can be distinguished. The O_{ad}/O_l ratio are shown in Table 3. The higher O_{ad}/O_l ratios were found on 3Mn/Al_2O_3-H_2O (1.7) and 3Mn/Al_2O_3-HNO_3 (1.8).

3.8 Temperature Programmed Reduction (TPR)

The TPR curves of catalysts are presented in Fig. 6. Catalysts present three reduction signals. The reduction sequence is probably: $Mn^{+4} \rightarrow Mn^{+3} \rightarrow Mn^{+2} + Mn^{+3} \rightarrow Mn^{+2}$. The first step $Mn^{+4} \rightarrow Mn^{+3}$, in majority of cases corresponding to a very small peak can create misunderstanding [29]. In general for supported manganese catalysts the first peak at low reduction temperature could be also attributed to the reduction of dispersed MnO_x species. The

Table 3 XPS results, isoelectric point (IEP) and apparent surface coverage (ASC)

Catalysts	Mn/Al	Oad/Ol	B.E. Mn2p (eV)	IEP	ASC
1Mn/Al_2O_3	0.17	1.0	641.2	6.9	83.8
3Mn/Al_2O_3	0.15	1.0	641.8	6.5	83.6
1Mn/Al_2O_3-H_2O	0.13	0.7	642.2	6.6	83.5
3Mn/Al_2O_3-H_2O	0.39	1.7	641.9	8.4	84.5
1Mn/Al_2O_3-HNO_3	0.15	1.0	641.6	7.2	83.8
3Mn/Al_2O_3-HNO_3	0.48	1.8	641.5	6.7	86.5

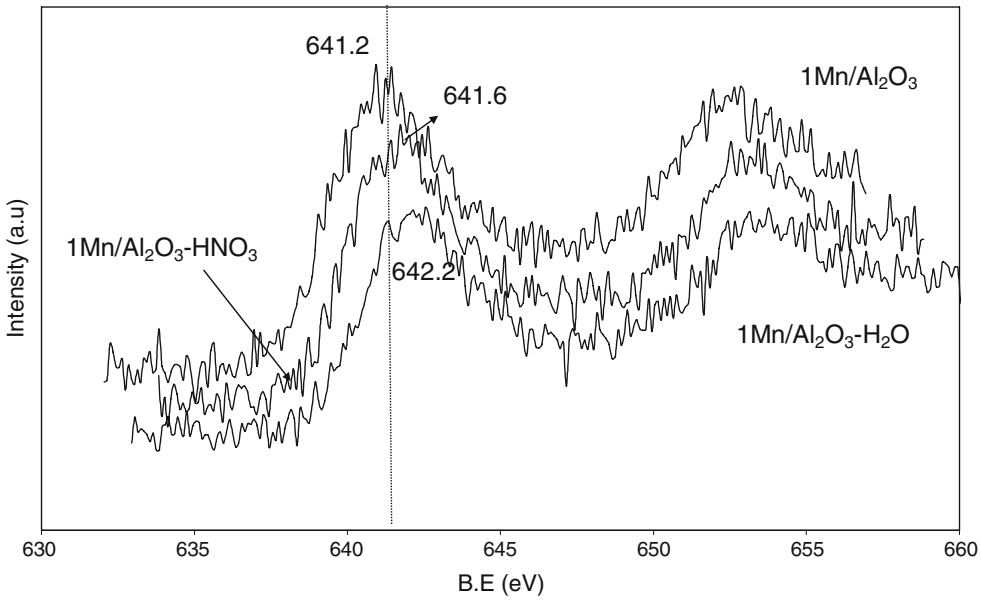

Fig. 5 XPS spectra of the Mn2p region

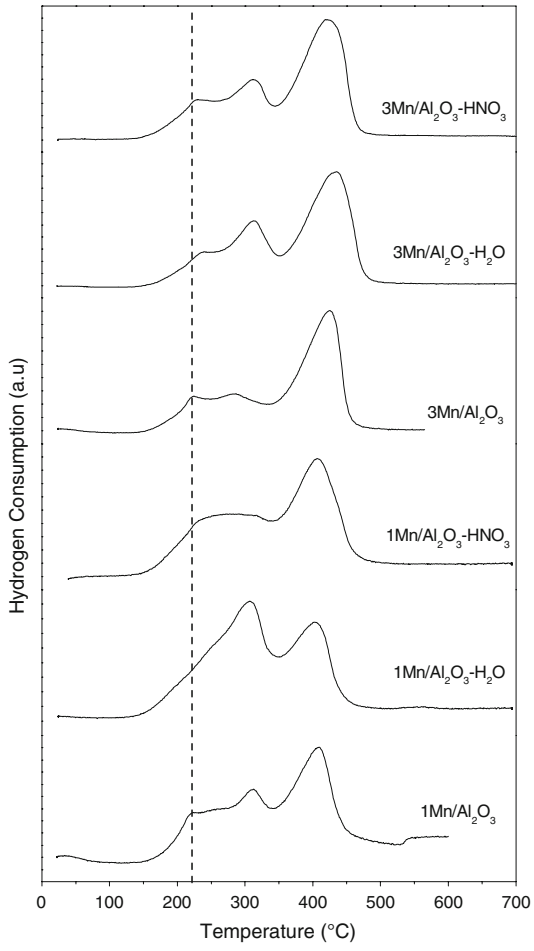

Fig. 6 Temperature programmed reduction profiles

reduction temperatures and the intensity ratios (1:2) of the second and the third peaks are similar to those reported for crystalline Mn_2O_3 [30, 31]. At low manganese loading it can be seen that the support treatments shift the first peak to higher temperatures. This shift is also observed for 3Mn/Al_2O_3-H_2O catalyst. We could assume that 1Mn/Al_2O_3-H_2O catalyst presents the higher amount of dispersed MnOx species, if we consider that the area under the curve is proportional to the amount of reducible species, and that the first peak is overlapped with the second. The third reduction signal shifts from 410 °C to around 420 °C and its intensity increases with the manganese loading but no important modifications with the support treatment is observed. The total H_2 consumption is converted into an average O/Mn atomic ratio (Table 2), assuming that the total reduction results in MnO. The O/Mn ratios of catalysts from the untreated supports are higher than the ones from treated supports. The increase in manganese loading decreased the O/Mn ratio of catalysts independently on the support.

3.9 Temperature Programmed Desorption of Oxygen (O_2-TPD)

Figure 7 shows the O_2-TPD results. Catalysts present a first signal between 150 and 350 °C. A second signal above 400 °C, which intensity increased for 1Mn/Al_2O_3 and 3Mn/Al_2O_3 catalysts is also observed. The first signal is generally denoted as α oxygen species and they correspond to oxygen species adsorbed on surface oxygen vacancies.

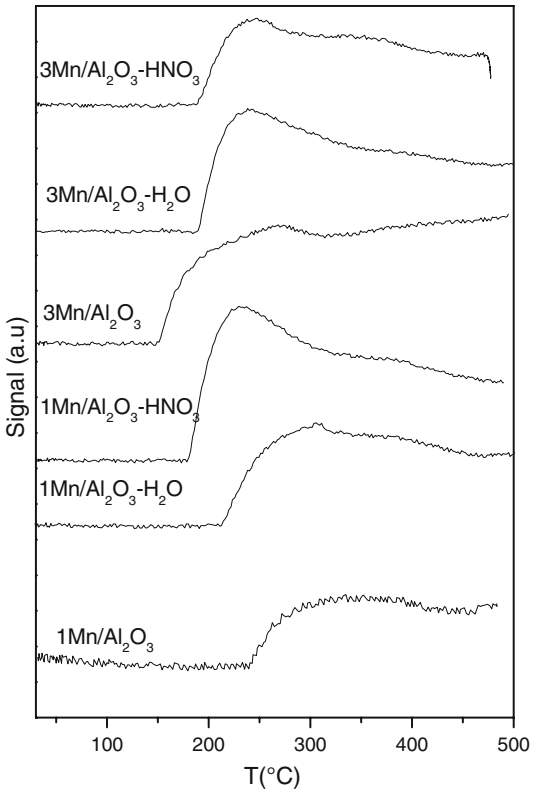

Fig. 7 Oxygen temperature programmed desorption curves

The second signal at higher temperatures is known as β oxygen species. This oxygen release from the oxide lattice [32, 33].

3.10 Catalytic Activity

The results of catalytic activity in ethanol and toluene combustion are presented in Fig. 8–11. It is clearly observed that the catalytic behavior of these catalysts is different depending on the VOC molecule studied. In ethanol combustion, the higher activity of catalysts supported on untreated Al_2O_3 was obtained with the higher manganese loading. Comparing T_{50} and T_{80} (reaction temperatures corresponding to 50% and 80% conversion, respectively), a difference of 15 °C is observed. In the case of catalysts supported on treated Al_2O_3 the influence of the manganese loading is less important. Considering the support treatment, it was observed that catalysts with low manganese loading were more active when the support was previously treated. The activity decreases in the following order: 1Mn/Al_2O_3-H_2O $\approx$ 1Mn/Al_2O_3-HNO_3 > 1Mn/Al_2O_3. At high manganese loading, higher conversions are obtained with catalysts prepared from treated supports specially at low reaction temperature, lower than 180 °C. Above this temperature, the conversion of ethanol on 3Mn/Al_2O_3 is higher than that on treated catalyst. Ethanol combustion occurs through an intermediate, acetaldehyde, on all the studied catalysts. The acetaldehyde yield varied widely as it is shown in Fig. 9, and for each catalyst goes through a maximum and then sharply decreases. The production of acetaldehyde, was higher when catalysts prepared from untreated supports were used. The maximum of acetaldehyde yield was reached at higher temperature on 1Mn/Al_2O_3-HNO_3 catalyst. 3Mn/Al_2O_3-HNO_3, 3Mn/Al_2O_3-

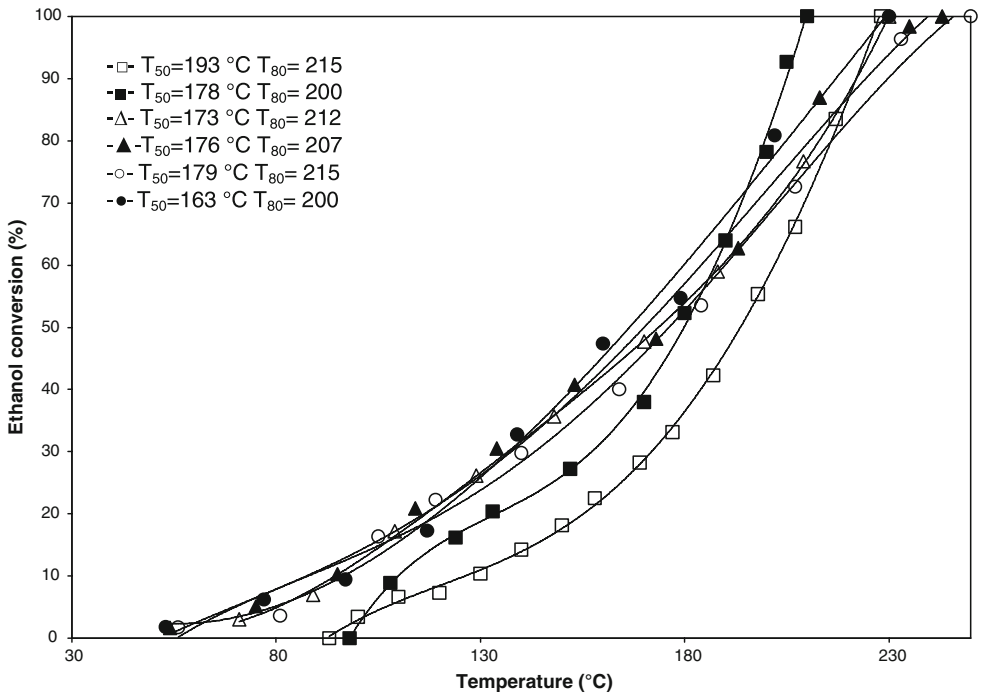

Fig. 8 Ethanol conversion as a function of reaction temperature for 1Mn/Al_2O_3 (□), 3Mn/Al_2O_3 (■), 1Mn/Al_2O_3-H_2O (Δ), 3Mn/Al_2O_3-H_2O (▲), 1Mn/Al_2O_3-HNO_3 (○), 3Mn/Al_2O_3-HNO_3 (●)

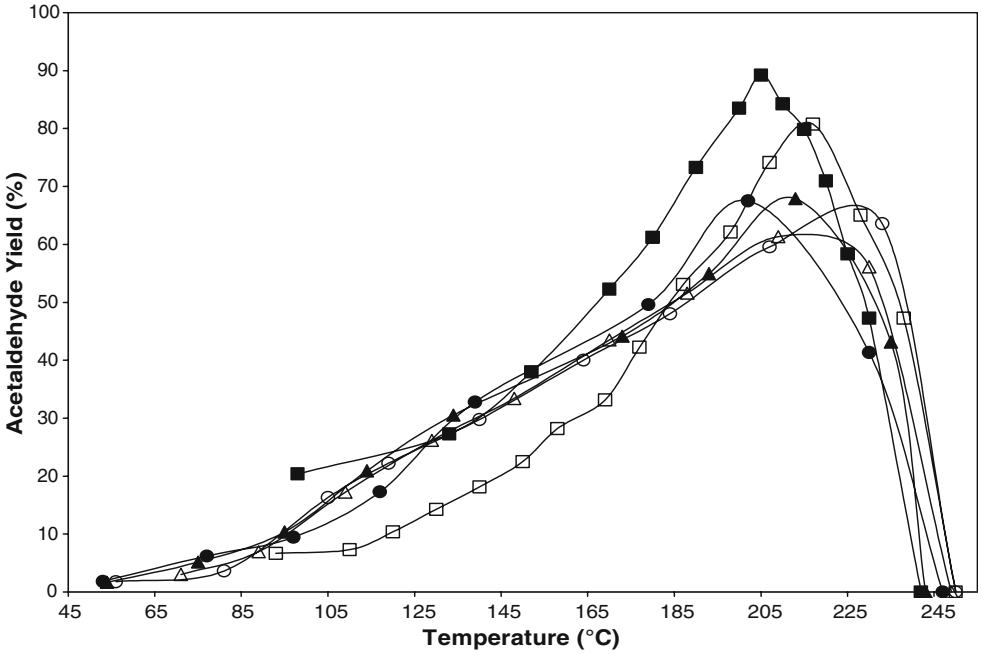

Fig. 9 Yield to acetaldehyde as a function of reaction temperature for $1Mn/Al_2O_3$ (□), $3Mn/Al_2O_3$ (■), $1Mn/Al_2O_3$-H_2O (Δ), $3Mn/Al_2O_3$-H_2O (▲), $1Mn/Al_2O_3$-HNO_3 (○), $3Mn/Al_2O_3$-HNO_3 (●)

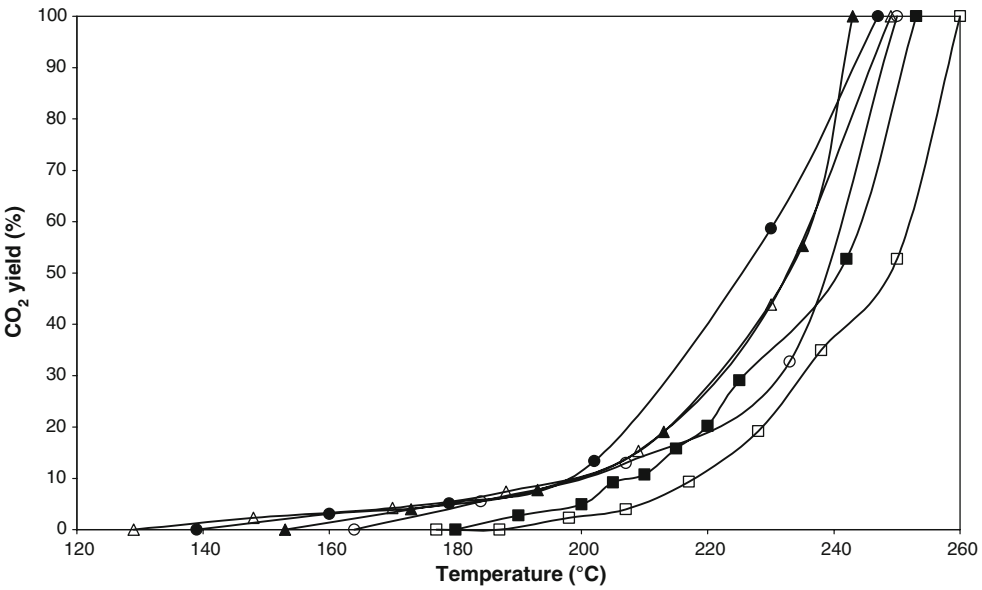

Fig. 10 Yield to CO_2 as a function of reaction temperature for $1Mn/Al_2O_3$ (□), $3Mn/Al_2O_3$ (■), $1Mn/Al_2O_3$-H_2O (Δ), $3Mn/Al_2O_3$-H_2O (▲), $1Mn/Al_2O_3$-HNO_3 (○), $3Mn/Al_2O_3$-HNO_3 (●)

H_2O, and $1Mn/Al_2O_3$-H_2O catalysts presented lower acetaldehyde yield and lower reaction temperatures than xMn/Al_2O_3 catalysts. In Fig. 10, CO_2 yield as a function of the reaction temperature is shown. As it can be observed catalysts prepared on treated supports are the most selective to total oxidation in the whole range of reaction temperature. Certainly, catalysts supported on treated alumina with a high manganese loading resulted the most active and selective catalysts in ethanol combustion.

In toluene combustion (Fig. 11), the catalytic activity increases with the increase of manganese loading independently on the support treatment. Comparing T_{50} and T_{80}, a difference of about 10 °C is observed for xMn/Al_2O_3 and xMn/Al_2O_3-H_2O, while a difference of 20 °C is observed in the case of xMn/Al_2O_3-HNO_3. Considering the support treatment, at low manganese loading, the most active catalyst resulted $1Mn/Al_2O_3$, while at higher manganese loading $3Mn/Al_2O_3$ and $3Mn/Al_2O_3$-HNO_3 presented a similar catalytic behavior and were more active than $3Mn/Al_2O_3$-H_2O catalyst. CO_2 was the only reaction product detected in toluene combustion reaction.

The supports did not give any combustion products. Only a small amount of diethyl ether was detected at 220 °C when ethanol combustion was evaluated.

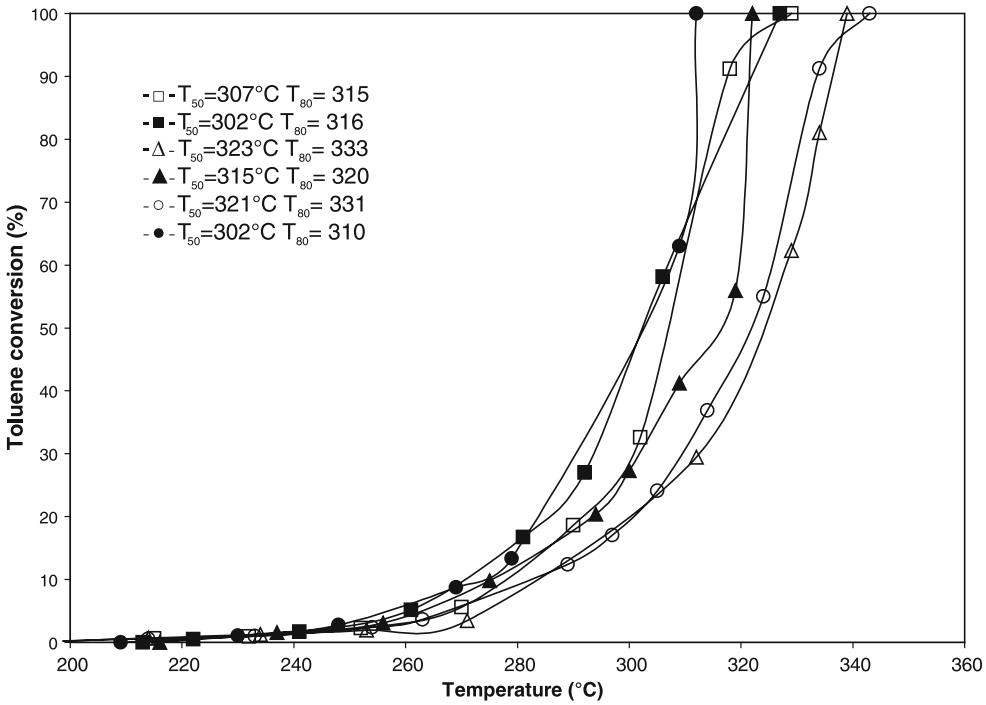

Fig. 11 Toluene conversion as a function of reaction temperature for 1Mn/Al_2O_3 (□), 3Mn/Al_2O_3 (■), 1Mn/Al_2O_3-H_2O (Δ), 3Mn/Al_2O_3-H_2O (▲), 1Mn/Al_2O_3-HNO_3 (○), 3Mn/Al_2O_3-HNO_3 (●)

4 Discussion

4.1 Effect of Support Treatments on Alumina Physicochemical Properties

The main objective when an active phase is deposited on a support oxide is to increase the exposed surface area. However, support nature and surface physicochemical properties could influence in the dispersion of the active phase and therefore, in the kind of surface specie formed. The anphoteric nature of alumina makes its surface chemistry very complex when it comes into contact with an acidic or basic aqueous solution [34]. In this work we used as support an alumina prepared following a very interesting method since a relatively high specific surface area (97.1 m^2/g) was obtained despite the high calcination temperature (1000 °C). By this way, a stable support which can be subject to high temperatures is obtained [35]. In fact the X-ray diffractogram of the Al_2O_3, (see Fig. 1), shows the transition phase θ-δ-Al_2O_3 (PDF 4–877 and 35–121). The structure of the original alumina was unchanged after the treatments. The modification of the alumina with different treatments has been evaluated in several cases giving interesting results [36, 37]. Treatments with water and nitric acid modified the textural properties of the original support. The surface area of water treated alumina decreases to 79.5 m^2/g. Probably the water treatment causes a blocking effect of the support pores causing a reduction of the specific surface area. It has been published [38] that the pores of the amorphous aluminas can be sealed by means of a hydrothermal treatment, which consists in immersing the alumina in boiling water or exposing it to water vapor. This produces dissolution of the alumina within the pores and a subsequent recrystallization near the pore mouth causing the sealing of the pores and in consequence, the decrease of the surface area. The necessary time to achieve the pore sealing is 2–3 min per each μm of thickness; however, it also depends on the original diameter of the pores. In this work, the treatment is carried on at room temperature, however, hydrotreatment could be considered since the support is dried at 100 °C in a vacuum stove after the treatment. The surface area of nitric acid-treated alumina increases to 106.3 m^2/g. This could be due to the acid attack that the surface suffers during the treatment. A dissolution of the solid was also observed. It is well known that the dissolution of the oxides depends on the solution pH, increases at acid pH, below the isoelectric point of the oxide and also increases in the alkaline region [39]. The pore volume and the pore mean diameter decreased after both treatments.

Beside the textural modifications, the support treatment can induce changes on the acid–base characteristics of the alumina. These changes are of great importance during the active phase impregnation process. Thus, the isoelectric point and the acidity, were determined.

Ming and Baker [40] revealed that the pH value of impregnating solution changed the interaction form of Co and silica support, the dispersion and reducibility of metal

Co. The support isoelectric point can affect the molecular structure of the active surface species during the catalysts preparation [41, 42]. At higher difference between the support isoelectric point and the precursor solution pH, a higher interaction of the active species with the support is obtained. The precursor used in this case is manganese acetate with a pH value of 6.5. Untreated alumina has an IEP of 7.9 and it increases when the support is treated with water or nitric acid (see Table 1). Thus, it could be assumed that a higher interaction of the manganese species with the treated supports would be obtained.

The total acidity and the acid strength distribution of the original alumina were modified by the treatments with water or nitric acid. The results of NH_3-TPD and IR-Py indicate that the treatment with water increases the total acidity and promotes a higher number of medium acid sites. As the increase of the IEP, these acidic properties could induce a stronger active phase–support oxide interaction. On the other hand, the treatment with nitric acid decreases the total acidity but increases the amount of the strong acid sites which also could generate a strong MnO*x*–support interaction.

In summary, treatments with water and acid nitric clearly modified the alumina physicochemical properties, mainly shown by changes in the porosity, surface area, isoelectric point and surface acidity. These changes could affect the interaction between support and active phase, dispersion and reducibility of the catalysts and therefore the catalytic activity.

4.2 Catalysts Characteristics

The characterization data of supported manganese oxide catalysts clearly demonstrate that support treatments induce the formation of manganese oxide species with different reducibility, dispersion and interaction active phase–support. For instance, the O/Mn ratio from H_2-TPR (Table 2), the Mn/Al surface atomic ratio and Mn2p binding energy from XPS (Table 3) were affected by the support treatments.

The temperature programmed reduction is a useful technique to obtain information about the supported active phase and its interaction with the support. Then, these results could help us to interpret the effect of the support treatments on the features of the supported manganese oxide phase. It is well know that the reduction curve of bulk Mn_2O_3 presents two reduction peaks [5, 31]. The presence of other signals at lower reduction temperatures would indicate the reduction of MnO*x* species in higher oxidation state (Mn^{4+}) or the presence of dispersed surface manganese oxide species [23]. The existence of manganese in oxidation state higher than 3 is not corroborated by the results of hydrogen consumption during the TPR. The O/Mn ratios are lower than the theoretical values expected for the total reduction of manganese +3 to +2, specially for the catalysts prepared from the treated aluminas. This would indicate that the initial average oxidation state of manganese is lower than 3 or that the Mn^{3+} is not completely reduced to Mn^{2+}. The former assumption could occur if the manganese oxide layer formed at the surface presented an oxygen deficit, while the incomplete reduction of Mn^{3+} to Mn^{2+} could occur if ions Mn^{3+} were stabilized in the lattice of the alumina. Studies on alumina supported manganese oxide catalysts calcined at different temperatures, [43] have shown that between 500 and 800 °C, solid solutions of Mn^{3+} in the alumina structure are formed due to the partial dissolution of manganese ions. Then, we can suggest that the signal at low temperature in the TPR profiles corresponds to dispersed surface manganese oxide species where manganese is mainly in oxidation state +3.

The maxima reduction temperatures of the dispersed surface manganese oxide species could indicate the interaction strength of these species with the support. The most interesting information is obtained from the catalysts with low manganese loading since, as detected by XRD, in those with high manganese loading a main part of manganese oxide is in the form of Mn_2O_3 crystallites. Thus, considering that higher reduction temperatures indicate stronger interaction of the reducible species with the support, we can postulate that the support treatments induce a stronger interaction manganese oxide species-alumina. The most important effect is obtained for the treatment with water. In line with this observation, the highest binding energy of Mn2p in the XPS spectra was detected for the $1Mn/Al_2O_3$-H_2O catalyst.

The origin of the stronger MnO_x-Al_2O_3 interaction could be explained by the modification of the acidic properties of the alumina after the treatments. The support acid sites can be considered as anchoring sites for the manganese and the acid strength of these sites could determinate the MnO*x*–support interaction strength, i.e., stronger acid sites originate stronger MnO*x*–support interactions. As concluded in Sect. 4.1, the higher amount of strong acid sites was observed on the Al_2O_3-HNO_3 while the treatment with water increased the amount of medium acid sites. Apparently, this would not explain the MnO*x*–support interaction deduced above. However, it must be taken into account that the total acidity of Al_2O_3-H_2O was noticeably higher than that of Al_2O_3-HNO_3. Thus, a higher amount of MnO*x* species could interact with acid sites on Al_2O_3-H_2O giving as result the increase of the interaction between surface MnO*x* species and the support in the following order: $Al_2O_3 < Al_2O_3$-$HNO_3 < Al_2O_3$-H_2O.

The support treatments apparently influence the dispersion of the surface manganese oxide phase in a contrary sense when low or high manganese loading is used.

Considering the Mn/Al atomic ratios from XPS or apparent surface coverage (ASC) results, higher manganese dispersion is obtained on the treated supports, for catalysts with high manganese loading. This tendency is in line with the increase of the isoelectric point (IEP) of the treated aluminas, i.e., the higher difference between the support IEP and the precursor solution pH leads to higher manganese oxide phase dispersion. However, for the catalysts with low manganese loading the manganese dispersion decreases in the order: $1Mn/Al_2O_3 > 1MnAl_2O_3\text{-}HNO_3 > 1Mn/Al_2O_3\text{-}H_2O$. In order to explain these results, it could be proposed that the stronger MnO*x*–support interaction of the catalysts prepared from treated alumina favors the dissolution of Mn^{3+} in the alumina structure giving surface Mn/Al atomic ratio lower than the expected ones.

Furthermore, it would be expected that the dissolution of Mn^{3+} could produce structural defects in the outer layer of the alumina support. This assumption is in agreement with the results of specific surface area (S_{BET}). When an oxide phase is supported on a porous support oxide, a decrease of the support S_{BET} is expected due to the pores blocking. For our catalysts with low manganese loading, the S_{BET} of untreated alumina decreased about 4.4% and that of $Al_2O_3\text{-}HNO_3$, around 1.7%. On the other hand, the S_{BET} of $1Mn/Al_2O_3\text{-}H_2O$ is around 33% higher than that of the $Al_2O_3\text{-}H_2O$ support. As it is said above, in particular for this treated alumina, higher amount of Mn ions could be dissolved in the alumina structure.

In summary, the supported manganese oxide layer is formed by dispersed surface manganese oxide species and crystalline Mn_2O_3. The increase of the support isoelectric point with the different treatments increases the dispersion of the manganese oxide phase. However, at low manganese loading, the increase of the acid sites strength on the treated aluminas induces a strong surface MnO*x* species–support interaction which favors the dissolution of Mn^{3+} in the alumina structure giving lower surface Mn/Al atomic ratio. Due to the stronger MnO*x*–treated alumina interaction, the dispersed surface manganese oxide species exhibit lower reducibity. This fact could be relevant for the catalytic activity.

4.3 Catalytic Performance and Oxygen Affinity

In order to evaluate the effect of the support treatment and the manganese loading on the catalytic behavior of catalysts, the samples were evaluated in total oxidation of ethanol and toluene. These molecules are considered to be in the extremes of the reactivity for combustion reactions [19]. The activity order depends on the nature of the molecule to be oxidized. In ethanol combustion, Fig. 8, the best catalytic performance is obtained with catalysts prepared from treated supports, specially at low reaction temperatures. Above 180 °C, catalysts prepared from untreated supports became more actives, showing a change in ethanol conversion curve slope, which could indicate a change in reaction mechanism. In fact at this temperature starts the production of CO_2 and acetaldehyde conversion. Ethanol in the feed can be oxidized in a sequential way to acetaldehyde and then to CO_2, however, direct oxidation of ethanol to CO_2 may also occur. It is clearly shown in Figs. 9 and 10 that ethanol oxidation on catalysts prepared from untreated supports follows the sequential way. On the other hand, catalysts prepared from treated supports with high manganese loading favour the direct oxidation of ethanol. In fact, these catalysts resulted the most active ones in ethanol total oxidation. These catalysts presented a stronger metal–support interaction which results in a higher manganese dispersion. The dispersed manganese oxide species, which are amorphous and defective species, are known to be very active in combustion reactions governed by a suprafacial mechanism. This mechanism is based in the interaction between surface oxygen (α-oxygen) and reactants, and it is operative at low temperature. These catalysts exhibit an oxygen desorption signal at around 230 °C which could be assigned to α-oxygen (Fig. 7). The higher capacity for adsorbing oxygen of $3Mn/Al_2O_3\text{-}H_2O$ and $3Mn/Al_2O_3\text{-}HNO_3$ is also deduced from the O_{ad}/O_l ratio determined by XPS (Table 2). Considering these results we could propose that ethanol total oxidation on supported manganese catalysts occurs by means of a suprafacial mechanism.

Another interesting feature is the small difference in T_{50} and T_{80}, about 4 °C, between $1Mn/Al_2O_3\text{-}H_2O$ and $3Mn/Al_2O_3\text{-}H_2O$ catalysts in ethanol oxidation, in spite of a lower O_{ad}/O_l ratio, lower manganese loading, and lower manganese dispersion on $1Mn/Al_2O_3\text{-}H_2O$. From Fig. 5 it can be observed that this catalyst presented a very intense reduction signal at about 300 °C. This signal is the result of the overlapping of two signals corresponding to the reduction of dispersed manganese oxides species and the first reduction step of crystalline Mn_2O_3. Evidently, the amount of surface MnO_x species in $1Mn/Al_2O_3\text{-}H_2O$ plays an important role in ethanol combustion. Furthermore, the high amount of Mn ions dissolved in the $Al_2O_3\text{-}H_2O$ support would produce a great number of defects on the catalyst surface. These defects could be active sites for the adsorption-activation of the reaction molecules and would be responsible of a higher catalytic activity.

On the other hand, there is a marked effect of the manganese loading in toluene combustion activity (Fig. 11). Catalysts with similar behavior like $3Mn/Al_2O_3$ and $3Mn/Al_2O_3\text{-}HNO_3$ were the most active ones. It is interesting to note that $1Mn/Al_2O_3$, the less active catalyst in ethanol combustion, presented a similar catalytic performance to $3Mn/Al_2O_3\text{-}H_2O$ in toluene combustion and it

was more active than the ones with low manganese loading prepared from the treated supports ($1Mn/Al_2O_3$-H_2O and $1Mn/Al_2O_3$-HNO_3). This catalytic behavior becomes difficult to explain from the characterization results, since it presented lower manganese loading, lower specific surface area, lower metal–support interaction and lower manganese dispersion. It seems that these conditions are not significant in toluene combustion. Evidently the oxidation of ethanol and toluene occur by different mechanisms.

Another mechanism proposed by Voorhoeve et al. [44] is the one which involves a redox cycle in which bulk oxygen (β-oxygen) migrates toward the surface becoming available for the oxidation of the substrate and it is replaced by gaseous oxygen through a Mars–van Krevelem mechanism. The oxygen mobility in the framework is associated to catalyst reducibility that can be studied by temperature programmed reduction. Therefore, a relationship between catalytic activity and reducibility may be established when catalyst undergoes a redox cycle. Toluene combustion seems to be roughly correlated with reducibility of the surface $MnOx$ species. TPR results indicate that the maxima reduction temperatures of the first signal increase in the same order as decreases their activity. The reduction temperature increases in the order: $3Mn/Al_2O_3 \cong 3Mn/Al_2O_3$-$HNO_3 < 1Mn/Al_2O_3 < 3Mn/Al_2O_3$-$H_2O < 1Mn/Al_2O_3$-$HNO_3 < 1Mn/Al_2O_3$-$H_2O$. Thereby, the better catalytic performance of catalysts with higher manganese loading could be explained if it is considered that toluene combustion proceeds through an intrafacial mechanism. Thus, the improvement in toluene combustion activity of $1Mn/Al_2O_3$ catalyst could be associated to the high reducibility that this catalyst presents. This is in agreement with the O_2-TPD results, where it can be observed that catalysts prepared from the untreated support exhibited an increase of the oxygen desorption signal above 400–420 °C, which may be considered as β-oxygen.

In conclusion, catalysts prepared from treated supports showed the best catalytic performance in ethanol combustion. At high manganese loading ($3Mn/Al_2O_3$-H_2O and $3Mn/Al_2O_3$-HNO_3 catalysts), this better catalytic performance was related to the high capacity for adsorbing oxygen. While at low manganese loading (mainly $1Mn/Al_2O_3$-H_2O), the great amount of dispersed surface manganese oxide species and/or the existence of surface defects were relevant in the catalytic activity. On the other hand, the reactivity of the catalysts in toluene combustion was roughly correlated with the reducibility of the surface manganese oxide species. On the basis of these observations, we conclude that the ethanol combustion occurs by a suprafacial mechanism, whereas the toluene combustion proceeds through an intrafacial mechanism.

5 Conclusions

Treatments with water and nitric acid clearly modified the alumina physicochemical properties, mainly shown by changes in the porosity, surface area, isoelectric point and surface acidity. The modification of the support surface properties increased the dispersion of the active phase and the interaction of the manganese oxide species with the support. At low manganese loading, the stronger surface manganese oxide–support interaction favours the dissolution of Mn^{3+} in the alumina structure giving lower Mn/Al atomic ratio. Due to the stronger $MnOx$–treated alumina interaction, the dispersed surface manganese oxide species exhibit lower reducibity.

Catalysts prepared from treated supports showed the best catalytic performance in ethanol combustion. At high manganese loading ($3Mn/Al_2O_3$-H_2O and $3Mn/Al_2O_3$-HNO_3 catalysts), this better catalytic performance was related to the high capacity for adsorbing oxygen. While at low manganese loading (mainly $1Mn/Al_2O_3$-H_2O), the great amount of dispersed surface manganese oxide species and/or the existence of surface defects were relevant in the catalytic activity. On the other hand, the reactivity of the catalysts in toluene combustion was roughly correlated with the reducibility of the surface manganese oxide species. On the basis of these observations, we conclude that the ethanol combustion occurs by a suprafacial mechanism whereas the toluene combustion proceeds through an intrafacial mechanism.

Acknowledgments The financial support from UNSL, CONICET and ANPCyT of Argentina is gratefully acknowledged. The authors also thank to Dr. M. Nazzarro for the XPS measurements.

References

1. Hodnett BK (2000) Heterogeneous catalytic oxidation. Wiley, New York, p 189,285
2. Gandia LM, Vicente MA, Gil A (2002) Appl Catal B 38:295
3. Merino NA, Barbero BP, Ruiz P, Cadús LE (2006) J Catal 240:245
4. Barbero BP, Gamboa JA, Cadús LE (2006) Appl Catal B 65:21
5. Morales MR, Barbero BP, Cadus LE (2007) Appl Catal B 74:1
6. Gélin P, Primet M (2002) Appl Catal B 39:1
7. Spivey JJ (1987) Ind Chem Res 26:2165
8. Spivey JJ, Butt JB (1992) Catal Today 11:465
9. Zwinkels MFM, Jaras SG, Menon PG, Griffin TA (1993) Catal Rev-Sci Eng 35:319
10. Trawczynski J, Bielak B, Mista W (2005) Appl Catal B 55:277
11. Lamaita L, Peluso MA, Sambeth JE, Thomas H, Minelli G, Porta P (2005) Catal Today 107–108:133
12. Lamaita L, Peluso MA, Sambeth JE, Thomas H (2005) Appl Catal B 61:114
13. Gallardo Amores JM, Armaroli T, Ramis G, Finocchio E, Busca G (1999) Appl Catal B 22:249
14. Fernandez-Lopez E, Sanchez-Escribano V, Resini C, Gallardo Amores JM, Busca G (2001) Appl Catal B 29:251

15. Zaki MI, Hasan MA, Pasupulety L, Kumasi K (1997) Thermochim Acta 303:171
16. Strohmeier BR, Hercules DM (1984) J Phys Chem 88:4922
17. Selwood PW, Moore TE, Ellis MJ (1949) J Am Chem Soc 71:693
18. Avila P, Montes M, Miró E (2005) Chem Eng J 11:11
19. O'Malley A, Hodnett BK (1999) Catal Today 54:349
20. Emeis CA (1993) J Catal 141:347
21. Damyanova S, Grange P, Delmon B (1997) J Catal 168:421
22. Gil-Llambias F, Escudey AM, Fierro JLG, Lopez Agudo A (1985) J Catal 95:520
23. Kapteijn F, Dick van Langeveld A, Moulijn JA, Andreini A, Vuurman M, Turek AM, Jehng J, Wachs I (1994) J Catal 150:94
24. Okamoto Y, Adachi T, Nagata K, Odawara M, Imanaka T (1992) Appl Catal A 82:199
25. Yamazoe N, Teraoka Y, Nakamura T (1981) Chem Lett 1767
26. Fierro JLG, Tejuca LG (1987) Appl Surf Sci 27:453
27. Fierro JLG (1990) Catal Today 8:153
28. Tejuca LG, Bell AT, Fierro JLG, Peña MA (1988) Appl Surf Sci 31:301
29. Stephan K, Hackenberger M, Wendt G (1999) Catal Today 54:23
30. Koh DJ, Chung JS, Kim YG, Lee JS, Nam IS, Moon SH (1992) J Catal 138:630
31. Stobbe ER, de Boer BA, Geus JW (1999) Catal Today 47:161
32. Voorhoeve RJH, Remeika JP, Freeland PE, Mattias BT (1972) Science 177:353
33. Seiyama T, Yamazoe N, Eguchi K (1985) Ind Eng Chem Prod Res Dev 24:19
34. Onoda GY, Casey A (1984) Ultra-structure processes of ceramics, glasses and composites. Wiley/Interscience, New York, p 374
35. Aguero FN, Barbero BP, Scian A, Cadús LE (2008) Catal Today 133–135:493
36. Zhang J, Chen J, Ren J, Sun Y (2003) Appl Catal A 243:121
37. Martin JA, Avila P, Suarez S, Yates M, Martin-Rojo AB, Barthelemy C, Martin JA (2006) Appl Catal B 67:270
38. Patermarakis G, Papandreadis N (1993) Electrochim Acta 36:1413
39. Kasprzyk-Hordern B (2004) Adv Interface Sci 110:19
40. Ming H, Baker BG (1995) Appl Catal A 123:23
41. Hu H, Wacho IE, Bare SR (1995) J Phys Chem 99:10897
42. Radhakrishnan R, Oyama ST, Chen JG, Asakura K (2001) J Phys Chem B 105:4245
43. Kochubeii DI, Kriventsov VV, Kustova GN, Odegova GV, Tsyrulnikov PG, Kudrja EN (1998) Kinet Katal 39:294
44. Voorhoeve RJH, Remeika JP, Johnson DW (1973) Science 180:62